Journal of Operation and Automation in Power Engineering

vol. XX, no. XX, Dec. 2022, Pages: XXXX (Proofed)

http://joape.uma.ac.ir

Maximizing the Generated Power of Wind Farms by Using Optimization Method

S.A. Abdul-Ameer[1,], A.K.J. Al-Nussairi[2], R. Khalid[3], J.K. Abbas[4], A.H.O. Al-Mansor[5]*

[1] *Ahl Al Bayt University, Karbala, Iraq.*
[2] *Al-Manara College for Medical Sciences, Amarah, Iraq.*
[3] *Medical Technical College, Al-Farahidi University, Baghdad , Iraq.*
[4] *AL-Nisour University College, Baghdad, Iraq.*
[5] *Department of Optical Techniques, Al-Zahrawi University College, Karbala, Iraq.*

Abstract— *In this study, the Particle Swarm Optimization (PSO) method was employed to optimize the anticipated energy yield of a wind farm. The architecture of a wind farm, including its location, height, and shadow reduction, is determined using the PSO algorithm based on the turbine height and rotor diameter. The proposed model presents two potential scenarios for the wind velocity and dispersion direction originating from a level wind location. The findings indicate that the optimization of the wind farm layout, encompassing factors such as location, height based on hub and rotor diameter of turbines, and maximum energy output, leads to a reduction in the shadow effect. This is in contrast to prior methodologies that optimized only one or two elements at a time. The wind farm's output power was observed to have a significant increase (ranging between 40% and 98%), despite having the same total number of wind turbines. This increase was attributed to the utilization of different hub heights and rotor diameters in comparison to the wind farm with different hub heights and rotor diameters, but the same number of wind turbines.*

Keywords—Wind Farm, Renewable Energy, Optimization.

1. INTRODUCTION

Worries about climate change resulting from the release of greenhouse gases into the atmosphere have compelled all nations to investigate strategies to limit their emissions [1], [2]. Energy is an important political tool for Western countries to exert pressure on other countries, especially the Middle East and Persian Gulf [3–5]. The European Union has decided to reduce its greenhouse gas emissions [6]. Wind turbines use wind energy to spin a generator and generate electricity [7]. These systems are often mounted on large towers to avoid interference from buildings, hills, and trees on the ground. Wind turbines are primarily utilized in the field of local electricity generation techniques that generate varying amounts of electricity [8], [9]. Owing to the vast amount of space they require, these methods are typically not employed in urban settings, but rather on farms. Numerous studies have been conducted in the field of wind turbines, with the majority of these studies focusing on increasing the efficiency of the generator, blades, rotor speed, and control of the electricity load of wind turbines, turbine farms, and energy and exergy analyses to decrease the cost of electricity [10], [11]. Wind power plants are advantageous because of their high efficiency, institutionalization of the technology used to harvest wind energy, and low cost of electricity produced [12]. It has been extended because wind blows most of the time, can create power on a large scale, and is more cost-effective than any of the existing methods for exploiting renewable energy sources in the power system. However, the increasing development of wind turbine manufacturing technology, which includes the reduction of the costs of developing and running wind turbines, has compelled nations to maximize their use of this energy [13].

In order to fully harness wind energy resources, it is imperative to employ sophisticated techniques in wind farm design [14]. Nowadays, wind power has emerged as a significant contributor to the global energy landscape, with the capacity to convert wind energy into various forms of useful energy, including electrical energy through wind turbines, mechanical energy in windmills or wind pumps, and propulsion in wind boats. This renewable energy source exhibits substantial annual production capabilities on a global scale [15]. The annual electricity production capacity can be enhanced with the extension of the wind farm [16].

Fuglsang and Madsen [17] who have investigated and assessed the methods for optimizing the wind turbine rotor and the design approaches based on numerical optimization and various scale models have contributed to the development of these turbines. Ozgner and Ozgener [18] analyzed the exergy and dependability of wind turbine systems at the University of Izmir in Turkey. Emami et al. [19] have determined the ideal location for wind turbine installation in wind farms by building a new code and implementing the genetic algorithm's goal function using software. Pope et al. [20] examined the energy efficiency and exergy of vertical and horizontal axis wind turbines. Asgari and Ehyaei [21] have utilized genetic and search algorithms to optimize wind turbines. Ashuri et al. [22] have developed a system-level strategy for optimizing the multi-string design of offshore wind turbines. Mortazavi et al. [23] employed the genetic algorithm to develop a Pareto optimal set of solutions for the geometric properties of airfoil sections for a 53-meter horizontally oriented wind turbine blade in a multi-objective study. Fakehi et al. [24] have utilized a combined renewable energy system based on wind, electrolysis, and PEM fuel cells in terms of conceptual model, energy

Received: 27 Jun. 2023
Revised: 10 sep. 2023
Accepted: 11 Sep. 2023
*Corresponding author:
E-mail: sabahauda79@gmail.com (S.A. AbdulAmeer)
DOI: 10.22098/JOAPE.2023.13226.2002
Research Paper

decomposition, and exergy reduction.

Shahata et al. [25] have examined the concept of turbine wells and the utilization of air column production changes over ocean waves to power a turbine. Wang et al. conducted research on wind turbine blades [26]. Ahmadi and Ehyaei [27] have examined and lowered the wind turbine's energy and exergy. This team first worked on the mathematical modeling of the wind turbine and then analyzed the energy and exergy with meteorological statistics based on the 6 main parameters of wind speed, cut-in speed which indicates the wind speed that must be blowing for the wind turbine to start moving, the Rated speed which corresponds to the maximum power produced by the wind turbine, and one of the other important speeds is the Furling speed, which if the wind speed reaches that value, the wind turbine will stop producing power.

In their study, Bai et al., [28] examined the effectiveness of an adaptive genetic algorithm in the context of displacement casting of multiple wind turbines. This investigation focused on a single-player reinforcement learning problem, wherein a Monte Carlo tree search was integrated into the evolutionary algorithm. Gua et al., [29] proposed a novel approach for optimizing wind farm design by utilizing an enhanced Gaussian model. Within this theoretical framework, the incorporation of local atmospheric stability was deemed a crucial input parameter, prompting the necessary modification of the wind power generation calculation method.

This study investigates the impact of shading on wind turbines, focusing on three conventional turbine types. The objective is to investigate two scenarios designed to optimize the turbines' energy production. Using the Particle Swarm Optimization (PSO) method, this research maximizes the anticipated energy output of a wind farm. The PSO algorithm calculates the architecture of the wind farm in terms of location, height, and shadow reduction based on the turbine height and rotor diameter. The proposed model provides two possibilities for wind speed and dispersion direction at a flat wind site.

2. MATERIALS AND MEHODS

The hypotheses and limitations of this research are as follows:

It is assumed that the wind farm has a rectangular shape as per the design. Introduction The turbines' spatial coordinates are represented by Cartesian coordinates (x, y), and the Euclidean distance between the turbine's location and a given point is calculated as the square root of the sum of the squares of the turbine's x and y coordinates, $i.e.$, $\sqrt{x^2 + y^2}$. The apparent inconsequentiality of the irregularity of the terrain may be deemed negligible, and the most advantageous resolution is demonstrated through the utilization of Cartesian coordinates (x_i, y_i) where i denotes the individual turbine, ranging from 1 to N (where N signifies the total number of turbines). Sufficient spacing between two turbines is necessary to mitigate hazardous loads on the turbines, including wind turbulence. The velocity distribution within the shaded region exhibits axial symmetry and uniformity. The expansion of the shaded region commences precisely at the rear of the turbine, while the free stream velocity remains constant and uniform. Furthermore, it is postulated that the velocity of shadow propagation exhibits a comparable shape. The determination of the additional parameter (α) of the bubble is conducted through experimental means and is contingent upon the underlying turbulence structure. The placement of turbines in a wind farm on a commercial scale is influenced by various operational factors, including but not limited to the local terrain, load-bearing capacity of the soil, and the design of farm roads. These factors are subject to regulation. The problem's mathematical model is comprised of two distinct components. The initial component pertains to the phenomenon of shadow effect, which has the potential to result in reduced power generation from turbines operating at lower elevations. The subsequent component pertains to the model for output power.

2.1. Shadow effect

The presence of neighboring wind turbines in a wind farm can result in a reduction in the efficiency of a given turbine, owing to the shadow effect. As wind flows through a wind turbine, a portion of its kinetic energy is imparted onto the blades of the turbine. The reduction of wind speed by the blades results in a volumetric expansion of mass accumulation located in front of the blades. In order to streamline the shadow model and disregard the influence of nearby turbulence intensity, the diffusion effect is postulated to be continuous and linear, as depicted in Fig. 1. The augmentation of the shadow effect is observed through the application of multiple shadows onto a singular wind turbine. The present model assumes a constant velocity of motion within the shadow.

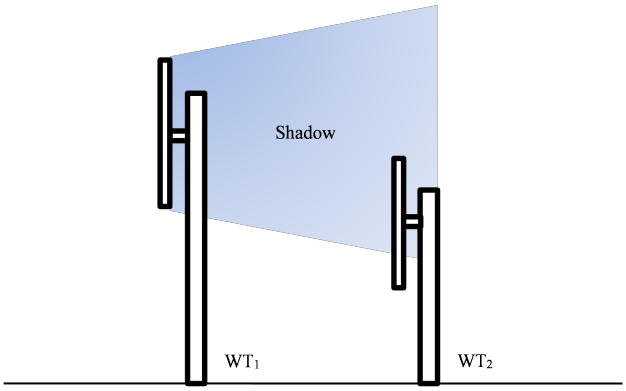

Fig. 1. Sketch of Shadow model.

The speed fraction of wind turbines is expressed by the following:

$$U_i = U_0 \left(1 - U_{\text{def}} \times (A_{\text{overtap}}/A)\right) \tag{1}$$

$$[U_0^j \left(Z_j\right) = \frac{u^*}{k} \ln\left(\frac{h_j}{z_0}\right) + \psi \tag{2}$$

where, U_0^j denotes the velocity of unrestricted flow ahead of the wind turbine, while u^* represents the friction velocity associated with the height of the turbine hub. The symbol J is used to represent the friction speed, and k refers to von Karman's constant. Additionally, the constant period is denoted by the symbol ψ. The value of ψ is determined by the stability of the conditions, with a value of zero indicating neutral conditions, a positive value indicating stable conditions, and a negative value indicating unstable conditions. It is assumed that the conditions in this study are neutral. The Equation (3) expressing the decrease in speed U_{def} is derived from the experimental values.

$$U_{def} = \frac{2a}{\left(1 + \alpha \frac{x}{r_r}\right)^2} \tag{3}$$

The symbol α denotes the constant that exhibits an upward trend in the bubble, while x represents the spatial displacement in the downstream direction from the wind turbine that generates the shadow. The value of alpha (α) can be computed by utilizing Equation (4). Given the utilization of wind turbines with varying hub heights in this study, it follows that alterations in the hub height hj will result in modifications to the value of α. The relationship between the shadow r_r and the constant governing bubble growth is established. Equation (5) can be utilized to ascertain the value of α and the distance x. Equation (7) serves as an initial explanation

of the correlation between the axial coefficient and the axial induction factor. This correlation is utilized in the computation of the lower rotor's radius, as demonstrated in Equation (6). The velocity u resulting from the merging of multiple shadows can be determined through the utilization of Equation (8). This equation involves the summation of the fractional kinetic energy of each individual shadow present at the given point, which ultimately yields the fractional kinetic energy of the mixed shadow [30]:

$$\alpha = \frac{0.5}{\ln\left(\frac{h_j}{Z_0}\right)} \tag{4}$$

$$r_1 = \alpha x + r \tag{5}$$

$$r_r = r\sqrt{(1-a)/(1-2a)} \tag{6}$$

$$a = \frac{1-\sqrt{1-C_T}}{2} \tag{7}$$

$$(1-u/U_0)^2 = \sum_{i=1}^{N}(1-U_i/U_0)^2 \tag{8}$$

2.2. Turbine power production model

The power produced by a wind turbine is calculated through the following equations [31]. Equation (9) calculates the output power of the wind turbine i^{th} with the wind speed V_i:

$$P_i = \frac{1}{2}\rho A V_i^3 C_p \tag{9}$$

where, ρ is the air density and PSO and C_p is the power coefficient (Equation (10)):

$$C_P = \frac{P}{\frac{1}{2}\rho A V^3} \tag{10}$$

The objective function used in the PSO to maximize the total output power of a wind farm is shown in Equation (11):

$$\text{Max P} = \sum_{i=1}^{N} P_i \tag{11}$$

The consideration of the rated wind speed of a wind turbine is an additional crucial aspect that warrants careful attention. In the event that the measured wind speed surpasses the wind turbine's designated rated wind speed, there will be no corresponding augmentation in power generation. When determining the output power, two scenarios are taken into account: (a) The wind speed observed is either equal to or exceeds the rated wind speed of the turbine, at which point the power output matches the installed capacity. (b) Conversely, the wind speed observed is lower than the speed at which the turbine is rated. The wind speed at which the turbine is rated, wherein the calculation of output power is determined by Equation (12):

$$P_i(U) = \begin{cases} 0 & U\langle U_c or U\rangle U_f \\ \frac{1}{2}\rho A U_i^3 C_p & U_c \le U \le U_r \\ P_{\text{rated}} & U_r \le U \le U_f \end{cases} \tag{12}$$

where U_c is the starting wind speed in the turbine (which is also called the starting speed of energy production), U_f is the cutting speed and U is the permissible limit of the wind speed. In other words, the stable power generation of the turbine is between U_r and U_f.

2.3. Particle Swarm Optimization (PSO) method

Research on the behavior of birds that has been conducted since 1990 indicates that all birds in a flock (flock group) that are searching for a good landing position are able to choose the optimal landing spot when that spot is held by one of its members [32]. There is congestion that has been identified. It is important to keep in mind that the conditions for surviving that will be present at a certain moment are the criteria that determine whether or not a place is suitable for landing [33]. These conditions will be used to make the decision. Some of these include the largest food supplies available and the lowest possible chance of being eaten by a predator. The issue of selecting the optimal point at which to touch down is one that pertains to optimization [34]. The group, swarm, or herd needs to locate the perfect landing spot, taking into account factors such as latitude and longitude, so that its members have the best possible chance of surviving the ordeal. In order to accomplish this, each bird in flight searches for a suitable landing spot and evaluates multiple places in terms of a wide variety of survival factors in order to discover the best landing zone, and this process is repeated until the best landing spot is identified.

The PSO technique, a non-deterministic search method for functional optimization, was proposed for the first time in 1995 [35]. In outer space, a flock of birds flies aimlessly in search of food. There is only one food item in the region that has been searched. In this method, each answer is referred to as a particle, PSO, and is analogous to a bird in the algorithm for the collective movement of birds. Each particle is allocated a merit value, which is determined by a merit function. Food symbolizes the target in the context of the bird movement model, and a particle's merit increases in proportion to how close it is to the target in the search space. Furthermore, each particle moves at its own velocity, which is governed by its own velocity. Each particle acts in accordance with the optimum particle behavior for the current state. It is still operating inside the parameters of the problem. At the start of the task, a set of particles is produced at random, and an attempt is made to find the best feasible solution through the process of updating the generations. The state of each particle is updated at each stage based on the two most recent values. When the particle is in the first position, it is in its most beneficial state. The point indicated, which is referred to as having the best nostalgia value for that particle and is represented by the notation pbest. Another best value used by the method is the best position that the particle population has obtained up to this point, which we refer to as $gbest$ (Fig. 2). Each particle calculates the value of the objective function in the position in the space in which it is presently located by combining information about its current location, the best location it has ever occupied in the past, and information about one or more of the group's best particles. Determines the path to be traveled. The current step of the algorithm is completed when everyone in the group completes the task at hand. These operations are repeated several times in order to achieve the desired result. As a result, based on its current speed, previous experience, and the experience of its neighbors, each particle moves towards m in the ideal point I space. The optimal point I space directs this movement. If the particle's position vector and velocity vector are supplied, the updated velocity and location of each particle, with v_i and l_i, are found by using Equations. (13) and (14) in the correct order:

$$\begin{aligned} v^i[t+1] &= wv^i[t] + \\ &c_1 rand_1\left(x^{i,pbest}[t] - x^i[t]\right) + \\ &c_2 rand_2\left(x^{gbest}[t] - x^i[t]\right) \end{aligned} \tag{13}$$

$$x^i[t+1] = x^i[t] + v^i[t+1] \tag{14}$$

$x^i[t]$ and $v^i[t]$ respectively indicating the speed and position of the i^{th} particle at time t. $x^{i,pbest}[t]$ and $x^{gbest}[t]$ the best personal position and the best collective position that the corresponding

particle has reached so far respectively. w is inertia coefficient which The lower its value, the faster the algorithm converges. $rand_1$ and $rand_2$ are random numbers with uniform distribution. c_1 and c_2 are personal learning and collective learning coefficient respectively. The objective function is the location of the wind turbine from the origin of coordinates defined in the model (Equation (15)):

$$f_{objective} = f\left(x, y, \sqrt{x^2 + y^2}\right) \tag{15}$$

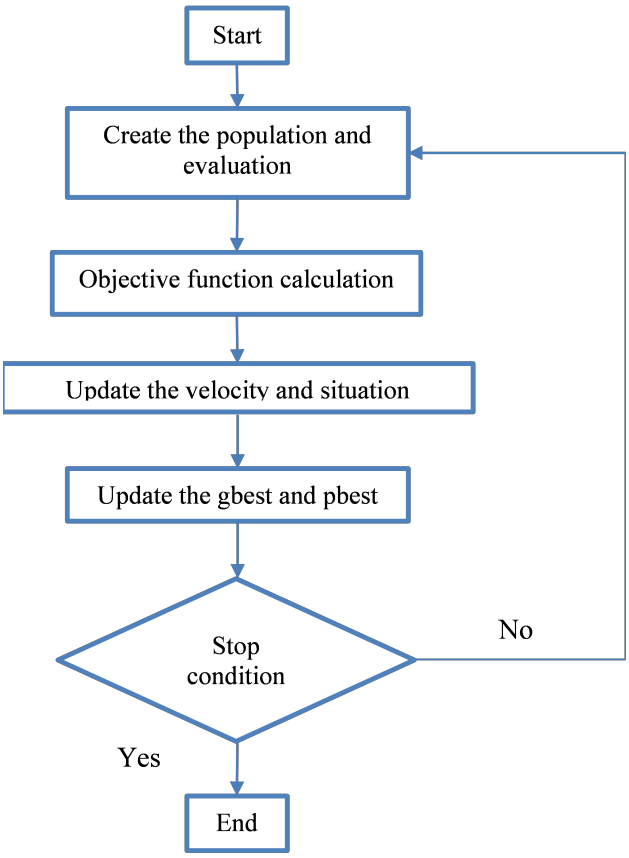

Fig. 2. PSO flowchart.

3. RESULTS AND DISCUSSION

The data utilized in this study were obtained from the daily average measurements of wind speed at a height of 10 meters above ground level throughout the year 2021. The aforementioned data were acquired from the Iraq Meteorological Organization and Seismology, which is dispersed across various locations within Iraq. The primary focus of this study was on the Amara stations situated in the southern region of Iraq, specifically at coordinates 47.10 longitude and 31.50 latitude. These stations can be described as having a predominantly flat topography with minimal variations in elevation [36].

As a result of the constraints imposed by the capacity for calculation, the dimensions of the wind farm are 1000 meters by 1000 meters, and it is composed of 2500 cells that are 20 meters by 20 meters. This layout may be seen in Fig. 2. The cell size ought to be sufficient for the purpose of determining possible locations for wind turbines. Throughout the area occupied by the wind farm, rather than installing wind turbines in the middle of each individual cell, all of the turbines are installed at the intersections of the grid (depicted in Fig. 3). The heights of the turbines are 60 and 75 meters, and their diameters are 30, 45, and 60 meters. The average wind speed is 15 meters per second, and the power output of the wind turbines is 700 kW. Both the power coefficient (Cp), which is defined as the ratio of the power extracted by the wind turbine relative to the energy available in the wind stream, and the thrust coefficient (Ct), which is defined as the ratio of the power extracted by the wind turbine relative to the energy available in the wind stream, are 0.45. As a result of the fact that two distinct turbine heights are being taken into account, there are two free stream speeds. As a result, the free stream speed at an elevation of 75 meters above ground level has been chosen as the reference wind speed. The wind speed that was utilized as a reference was employed in the calculation to determine the velocity of the free stream at a distance of 60 meters. This study takes into account two different sets of wind conditions, with the reference wind speed remaining constant across both sets at 13 meters per second. In the first possible situation, we are assuming that the wind is blowing from the east to the west. In the second possible outcome, the direction of the wind is segmented into 24 different directions, with an increase of 15 degrees between each pair of adjacent directions. We will assume that the probability of each possible direction is equal. While we are using the PSO method, it is important to emphasize that this method does not definitely guarantee that the overall optimal solution will be found.

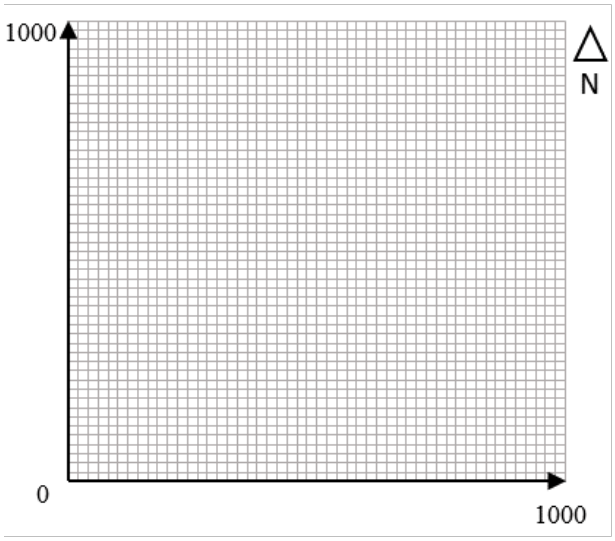

Fig. 3. Wind farm domain.

The first scenario is performed with constant wind speed and direction. The wind farm has a set number of wind turbines. In this case, the minimum spacing between turbines is 40 meters. The wind farm's output power is calculated using wind turbines with hub heights of 75 m and 50 m and rotor diameters of 30 m and 60 m.

The PSO is used to do the optimization using a randomly generated initial population of wind farm layouts. Fig. 3 displays the best wind farm architecture for this situation. Wind turbines, in actuality, are equally directed toward the wind. Fig. 4-(a) shows 50 wind turbines with a maximum output power of 23 MW. Fig. 4-(b) depicts how the curve of its objective function varies with algorithm iteration. Table 1 shows the origin of the wind turbine in the computational domain.

Because wind turbines in the first row are not affected by shadowing and often produce greater output power than other turbines, the maximum number of wind turbines that are permitted is positioned in the eastern row. As can be seen in 4-(a), the algorithm selected wind turbines with a higher turbine height in order to maximize output power while simultaneously minimizing the effect of shadows. However, the output power of the wind

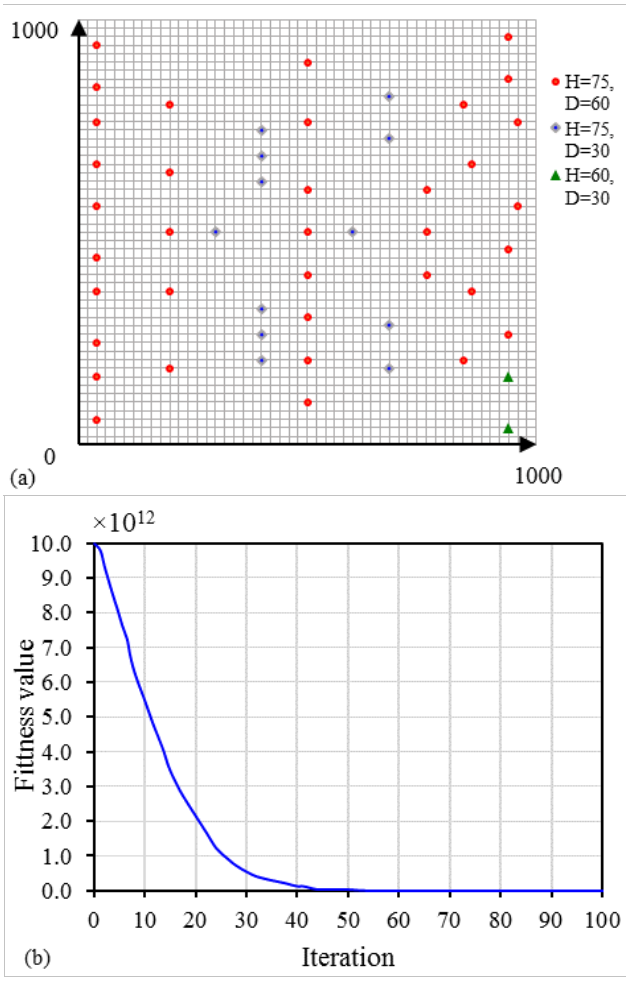

Fig. 4. a) the optimal arrangement created by PSO and b) the objective value vs iteration in PSO approach for scenario 1.

farm is not directly proportional to the diameter of the turbines' rotors, and the goal of the intelligent algorithm is to minimize both sizes of the rotor diameter. Given these conditions, the power of the wind farm has increased as the height of the turbine has increased. According to the findings, simultaneous optimization of the location, hub height, and rotor diameter produces significantly better results in terms of improving the output power of the wind farm than optimization of the location and hub height alone. This is the case even when comparing optimization of the location and hub height separately.

It has been determined that 50 turbines with varying hub heights will produce a total output power of 15 MW. According to this study, the power output of 50 turbines with the same hub height is MW 45, while the power output of 50 turbines with varying hub heights and rotor diameters is MW 48. Both of these results are based on 50 turbines.

Scenario $2's$ wind conditions include variable wind directions and a constant wind speed. There will be no directional shift because it is assumed that all directions have an equal chance of occurring. Furthermore, the lack of direction prohibits the formation of the ideal configuration of manifolds that produces the same or nearly equivalent output power. When the wind direction changes, one wind turbine may be in the shade of another, jeopardizing the optimal configuration's outcomes. It is calculated using wind turbines with rotor diameters of 45 and 60 meters, respectively, and hub heights of 75 and 60 meters.

Fig. 5-(a) illustrates the configuration of the wind farm that is optimal for the scenario that has been presented, and Fig. 5-(b) depicts the variation of the objective function that occurs throughout each iteration of the algorithm. The x and y coordinates of a wind turbine are listed in Table 2, along with the distances that these coordinates represent from the starting point. The wind farm is made up of fifty turbines and has a combined power output of 25.5 $megawatts$ (MW). The turbines have an output power that can reach a maximum of 75 meters, and there are four turbines that each have a hub height of 60 meters and a rotor diameter that also measures 60 meters. The power output of the system is capable of reaching a maximum of 15 $megawatts$ when operating at full capacity. It is interesting to note that wind turbines have a strong preference for positioning themselves around the central axis of the wind farm, which makes it easier for them to function. The data are presented in Fig. 5-(a), and it can be seen that the sides with a lower shadow impact exhibit a relatively greater output power. This can be seen by comparing these sides to one another. The program implemented the utilization of wind turbines with increased hub height and rotor diameter in order to enhance the output power and mitigate the effect of shadowing. The power output of the

Table 1. Wind turbine location and origin scenario 1.

WT type	WT ID	x	y	$\sqrt{x^2+y^2}$
H=60, D=60	1	40	940	940.85
	2	160	940	953.52
	3	260	940	975.29
	4	460	940	1046.52
H=75, D=60	5	860	940	1274.05
	6	960	940	1343.58
	7	900	500	1029.56
	8	760	500	909.73
	9	600	500	781.02
	10	500	500	707.11
	11	400	500	640.31
	12	800	840	1160.00
	13	200	840	863.48
	14	760	960	1224.42
	15	560	960	1111.40
	16	660	860	1084.07
	17	360	860	932.31
	18	500	760	909.73
	19	600	760	858.84
	20	600	760	968.30
	21	300	500	583.10
	22	200	500	538.52
	23	100	500	509.90
	24	60	40	72.11
	25	160	40	164.92
	26	240	40	243.31
	27	360	40	362.22
	28	440	40	441.81
	29	560	40	561.43
	30	660	40	661.21
	31	760	40	761.05
	32	840	40	840.95
	33	940	40	940.85
	34	800	200	824.62
	35	640	200	670.52
	36	500	200	538.52
	37	360	200	411.83
	38	180	200	269.07
H=75, D=30	39	200	400	447.21
	40	260	400	477.07
	41	320	400	512.25
	42	500	300	583.10
	43	620	400	737.83
	44	680	400	788.92
	45	740	400	841.19
	46	180	680	703.42
	47	280	680	735.39
	48	720	680	990.35
	49	820	680	1065.27
	50	500	600	781.02

wind farm has been increased thanks to the implementation of hub height elevation and rotor extension. These changes were made in response to the conditions that were present. It is of the utmost importance to recognize that the configuration of the farm, which includes its geographical placement and the characteristics of the turbines chosen, is dependent upon the host state. This is because of the variable wind patterns and the variation in the minimum distance between turbines.

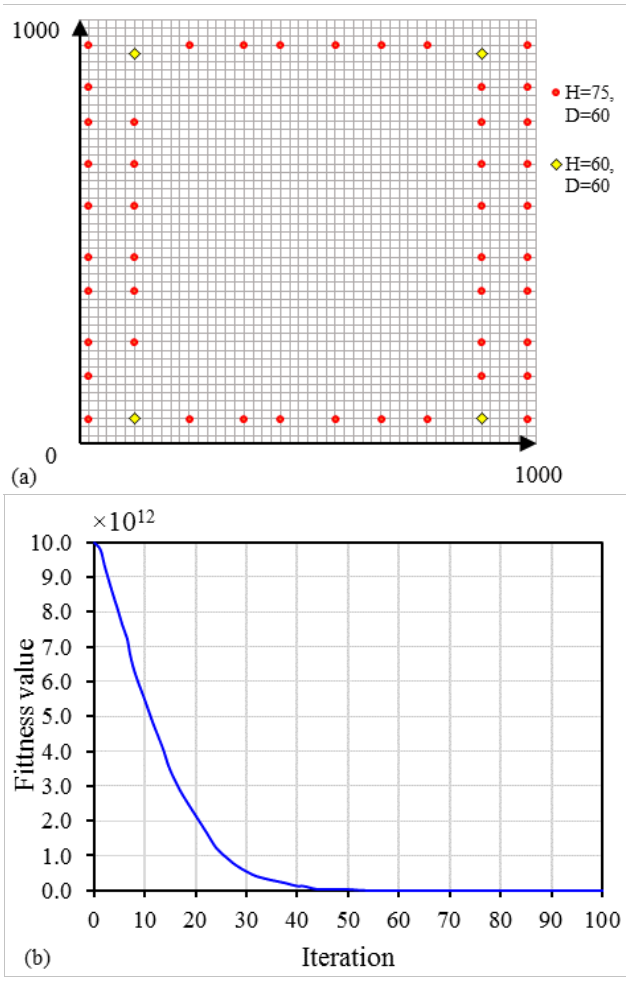

Fig. 5. the optimal arrangement created by PSO and b) the objective value vs iteration in PSO approach for scenario 2.

Table 2. Wind turbine location and origin scenario 2.

WT type	WT ID	x	y	$\sqrt{x^2+y^2}$
H=60, D=60	1	60	880	882.04
	2	920	120	927.79
	3	60	120	134.16
	4	920	880	1273.11
H=75, D=60	5	60	20	63.25
	6	160	20	161.25
	7	240	20	240.83
	8	360	20	360.56
	9	440	20	440.45
	10	560	20	560.36
	11	660	20	660.30
	12	760	20	760.26
	13	840	20	840.24
	14	940	20	940.21
	15	60	980	981.84
	16	160	980	992.98
	17	240	980	1008.96
	18	360	980	1044.03
	19	440	980	1074.24
	20	560	980	1128.72
	21	660	980	1181.52
	22	760	980	1240.16
	23	840	980	1290.74
	24	940	980	1357.94
	25	840	880	1216.55
	26	240	120	268.33
	27	360	120	379.47
	28	440	120	456.07
	29	560	120	572.71
	30	660	120	670.82
	31	760	120	769.42
	32	760	880	1162.76
	33	660	880	1100.00
	34	940	240	970.15
	35	940	360	1006.58
	36	940	440	1037.88
	37	940	560	1094.17
	38	940	660	1148.56
	39	940	760	1208.80
	40	560	880	1043.07
	41	440	880	983.87
	42	60	240	247.39
	43	60	360	364.97
	44	60	440	444.07
	45	60	560	563.21
	46	60	660	662.72
	47	60	760	762.36
	48	360	880	950.79
	49	160	880	894.43
	50	240	880	912.14

4. CONCLUSION

The present study employed the Particle Swarm Optimization (PSO) method to examine the impacts associated with the utilization of non-uniform wind turbines. This study encompassed the optimization of various factors, including space-time coordination, hub height, and turbine rotor diameter. Rather than examining the collective influence of all elements on enhancing wind farm layout and maximizing output power, the focus of the study has been on optimizing wind farm architecture to maximize output power. The objective has been effectively achieved through the utilization of wind turbines featuring either varying hub heights while maintaining the same rotor diameter, or a combination of both differing hub heights and rotor diameters. Based on statistical data, there has been a notable increase in the power output generated by the wind farm. There was a notable enhancement in the width of the path and the positioning of the wheel's center. This improvement was observed in comparison to a wind farm with an equivalent number of wind turbines, where the improvement amounted to approximately 40%. Furthermore, when compared to a wind farm with the same diameter but differing hub heights, the improvement reached approximately 98%. The total number of wind turbines remains constant. The wind farm is designed with an optimal layout consisting of a total of 50 turbines, which collectively generate a power output of $25.5\ MW$.

The strategies described in this article are not restricted to wind turbines that have two rotor diameters, two hub heights, and discrete values. One can use a real coded PSO to signal the number of variables, their placement, the height of the hub, and the diameter of the rotor all at the same time. As long as the shadow model remains stable, this method can also be utilized for the construction of a variety of wind farms. One of the benefits of utilizing wind turbines in a wind farm that have varying hub heights and rotor diameters is the reduction in the influence that shadows have. Moreover, the diameter of the rotor should be significantly reduced.

REFERENCES

[1] A. Molajou, A. Afshar, M. Khosravi, E. Soleimanian, M. Vahabzadeh, and H. A. Variani, "A new paradigm of water, food, and energy nexus," *Environ. Sci. Pollut. Res.*, pp. 1–11, 2021.

[2] A. Molajou, P. Pouladi, and A. Afshar, "Incorporating social system into water-food-energy nexus," *Water Resour. Manage.*, vol. 35, pp. 4561–4580, 2021.

[3] M. Koruzhde and R. W. Cox, "The transnational investment bloc in us policy toward saudi arabia and the persian gulf," *Cl. Race Corporate Power*, vol. 10, no. 1, 2022.

[4] M. Koruzhde, "The iranian crisis of the 1970s-1980s and the formation of the transnational investment bloc," *Cl. Race Corporate Power*, vol. 10, no. 2, 2022.

[5] M. Koruzhde and V. Popova, "Americans still held hostage: a generational analysis of american public opinion about the iran nuclear deal," *Polit. Sci. Q.*, vol. 137, no. 3, pp. 511–537, 2022.

[6] A. Matani and A. Mali, "Blending methanol as a renewable fuel in automotive industries towards minimizing vehicular air pollution," *Int. J. Recent Technol. Eng.*, vol. 8, no. 3, pp. 5496–5498, 2019.

[7] A. R. Nejad, J. Keller, Y. Guo, S. Sheng, H. Polinder, S. Watson, J. Dong, Z. Qin, A. Ebrahimi, R. Schelenz, *et al.*, "Wind turbine drivetrains: state-of-the-art technologies and future development trends," *Wind Energy Sci. Discuss.*, vol. 2021, pp. 1–35, 2021.

[8] A. H. Rajpar, I. Ali, A. E. Eladwi, and M. B. A. Bashir, "Recent development in the design of wind deflectors for vertical axis wind turbine: A review," *Energ.*, vol. 14, no. 16, p. 5140, 2021.

[9] H. Mousavi-Sarabi, M. Jadidbonab, and B. Mohammadi Ivatloo, "Stochastic assessment of the renewable–based multiple energy system in the presence of thermal energy market and demand response program," *J. Oper. Autom. Power Eng.*, vol. 8, no. 1, pp. 22–31, 2020.

[10] F. Azlan, J. Kurnia, B. Tan, and M.-Z. Ismadi, "Review on optimisation methods of wind farm array under three classical wind condition problems," *Renewable Sustainable Energy Rev.*, vol. 135, p. 110047, 2021.

[11] A. Jasemi and H. Abdi, "Probabilistic multi-objective optimal power flow in an ac/dc hybrid microgrid considering emission cost," *J. Oper. Autom. Power Eng.*, vol. 10, no. 1, pp. 13–27, 2022.

[12] A. Genus and M. Iskandarova, "Transforming the energy system? technology and organisational legitimacy and the institutionalisation of community renewable energy," *Renewable Sustainable Energy Rev.*, vol. 125, p. 109795, 2020.

[13] M. D. Leiren, S. Aakre, K. Linnerud, T. E. Julsrud, M.-R. Di Nucci, and M. Krug, "Community acceptance of wind energy developments: Experience from wind energy scarce regions in europe," *Sustainability*, vol. 12, no. 5, p. 1754, 2020.

[14] N. Aravindhan, M. Natarajan, S. Ponnuvel, and P. Devan, "Performance analysis of shrouded invelox wind collector in the built environment," *Sci. Technol. Built Environ.*, vol. 28, no. 5, pp. 677–689, 2022.

[15] A. Shahdadi, B. ZM-Shahrekohne, and S. Barakati, "Analyzing impacts of facts devices in dealing with short-term and long-term wind turbine faults," *J. Oper. Autom. Power Eng.*, vol. 7, no. 2, pp. 206–215, 2019.

[16] F. Porté-Agel, M. Bastankhah, and S. Shamsoddin, "Wind-turbine and wind-farm flows: A review," *Boundary Layer Meteorol.*, vol. 174, no. 1, pp. 1–59, 2020.

[17] P. Fuglsang and H. A. Madsen, "Optimization method for wind turbine rotors," *J. Wind Eng. Ind. Aerodyn.*, vol. 80, no. 1-2, pp. 191–206, 1999.

[18] O. Ozgener and L. Ozgener, "Exergy and reliability analysis of wind turbine systems: a case study," *Renewable Sustainable Energy Rev.*, vol. 11, no. 8, pp. 1811–1826, 2007.

[19] A. Emami and P. Noghreh, "New approach on optimization in placement of wind turbines within wind farm by genetic algorithms," *Renewable Energy*, vol. 35, no. 7, pp. 1559–1564, 2010.

[20] K. Pope, I. Dincer, and G. Naterer, "Energy and exergy efficiency comparison of horizontal and vertical axis wind turbines," *Renewable energy*, vol. 35, no. 9, pp. 2102–2113, 2010.

[21] E. Asgari and M. Ehyaei, "Exergy analysis and optimisation of a wind turbine using genetic and searching algorithms," *Int. J. Exergy*, vol. 16, no. 3, pp. 293–314, 2015.

[22] T. Ashuri, M. B. Zaaijer, J. R. Martins, G. J. Van Bussel, and G. A. Van Kuik, "Multidisciplinary design optimization of offshore wind turbines for minimum levelized cost of energy," *Renewable energy*, vol. 68, pp. 893–905, 2014.

[23] S. M. Mortazavi, M. R. Soltani, and H. Motieyan, "A pareto optimal multi-objective optimization for a horizontal axis wind turbine blade airfoil sections utilizing exergy analysis and neural networks," *J. Wind Eng. Ind. Aerodyn.*, vol. 136, pp. 62–72, 2015.

[24] A. H. Fakehi, S. Ahmadi, and M. R. Mirghaed, "Optimization of operating parameters in a hybrid wind–hydrogen system using energy and exergy analysis: Modeling and case study," *Energy Convers. Manage.*, vol. 106, pp. 1318–1326, 2015.

[25] A. S. Shehata, K. M. Saqr, Q. Xiao, M. F. Shehadeh, and A. Day, "Performance analysis of wells turbine blades using the entropy generation minimization method," *Renewable Energy*, vol. 86, pp. 1123–1133, 2016.

[26] L. Wang, A. Kolios, T. Nishino, P.-L. Delafin, and T. Bird, "Structural optimisation of vertical-axis wind turbine composite blades based on finite element analysis and genetic algorithm," *Compos. Struct.*, vol. 153, pp. 123–138, 2016.

[27] A. Ahmadi and M. Ehyaei, "Exergy analysis of a wind turbine," *Int. J. Exergy*, vol. 6, no. 4, pp. 457–476, 2009.

[28] F. Bai, X. Ju, S. Wang, W. Zhou, and F. Liu, "Wind farm layout optimization using adaptive evolutionary algorithm with monte carlo tree search reinforcement learning," *Energy Convers. Manage.*, vol. 252, p. 115047, 2022.

[29] N. Guo, M. Zhang, B. Li, and Y. Cheng, "Influence of atmospheric stability on wind farm layout optimization based on an improved gaussian wake model," *J. Wind Eng. Ind. Aerodyn.*, vol. 211, p. 104548, 2021.

[30] M. Khanali, S. Ahmadzadegan, M. Omid, F. Keyhani Nasab, and K. W. Chau, "Optimizing layout of wind farm turbines using genetic algorithms in tehran province, iran," *Int. J. Energy Environ. Eng.*, vol. 9, pp. 399–411, 2018.

[31] R. Zahedi, A. Ahmadi, and M. Sadeh, "Investigation of the load management and environmental impact of the hybrid cogeneration of the wind power plant and fuel cell," *Energy Rep.*, vol. 7, pp. 2930–2939, 2021.

[32] D. Wang, D. Tan, and L. Liu, "Particle swarm optimization algorithm: an overview," *Soft Comput.*, vol. 22, pp. 387–408, 2018.

[33] F. Marini and B. Walczak, "Particle swarm optimization (pso). a tutorial," *Chemom. Intell. Lab. Syst.*, vol. 149, pp. 153–165, 2015.

[34] V. Nourani, N. Rouzegari, A. Molajou, and A. H. Baghanam, "An integrated simulation-optimization framework to optimize the reservoir operation adapted to climate change scenarios," *J. Hydrol.*, vol. 587, p. 125018, 2020.

[35] J. Kennedy and R. Eberhart, "Particle swarm optimization in: Proceedings of icnn'95-international conference on neural networks, 1942–1948," *IEEE, Perth, WA, Australia*, 1995.

[36] B. M. Lateef, A. I. Al-Tmimi, and O. I. Abdullah, "Design and implementation of wind energy analysis tool (weatb) in iraq," in *AIP Conf. Proc.*, vol. 2144, AIP Publishing, 2019.